Electroformation of Giant Vesicles from an Inverse Phase Precursor

Omar Mertins,[†*] Nádya P. da Silveira,[‡] Adriana R. Pohlmann,[‡] André P. Schröder,[†] and Carlos M. Marques[†]
[†]Institut Charles Sadron, UPR22, Centre National de la Recherche Scientifique, Université de Strasbourg, Strasbourg, France; and [‡]Programa de Pos-Graduação em Química, Universidade Federal do Rio Grande do Sul, Porto Alegre, Brazil

ABSTRACT We discuss a simple modification of the well-known method of giant vesicle electroformation that allows for a direct addition of water-soluble species to the phospholipid bilayers. Using this modified method, we prepare phospholipid vesicles decorated with chitosan, a water-soluble polysaccharide currently investigated for potential pharmacological applications. We find that the method allows this polysaccharide with primary amino groups on every glucose subunit to be tightly bound to the membrane, rather than simply being encapsulated.

INTRODUCTION

Phospholipid bilayers are amphiphilic members of the large family of self-assembling systems, but they can seldom be prepared by ordinary direct self-assembly. Indeed, molecular dissolution in water cannot be directly achieved for most of the phospholipids of practical interest: even when small aggregates are obtained by injecting energy into the dissolution process, the extremely small values of the associated critical micellar concentrations prevent the relaxation of the system toward its equilibrium configuration. In practice, small unilamellar liposomes and large unilamellar vesicles need to be prepared by several successive steps, which are designed to circumvent the limitations of low solubility. A preparation step common to many methods involves the dissolution of the phospholipids in a volatile solvent, from which a substrate coated with a phospholipid thin film is obtained. Exposure of this preordered film to an aqueous solution followed by gentle hydration (1,2) or different methods of injection of mechanical or electrical energy eventually leads to the transfer of the preformed bilayers into the solution. For instance, the formation of small unilamellar vesicles (SUVs), with sizes between a few tens and 100 nm, can be obtained by ultrasonication or temperature elevation in phospholipids surfactant mixtures (3–5). Sandwiching the precursor film and the growth solution between two electrodes and then applying an electrical voltage typically induce giant unilamellar vesicles (GUVs), with diameters as large as 100 μm (6–8). Composite bilayer structures that also incorporate other species can be formed by the same method if both the phospholipids and those species are soluble in a common volatile solvent or solvent mixture. This may easily be achieved for organic molecules, but only rarely for water-soluble materials. In this last important case, an alternative method exists for the formation of SUVs and/or large unilamellar vesicles (LUVs). A small amount of an aqueous solution containing the water-soluble species is added to the volatile organic solvent, which results in an inverted phase of small water droplets dispersed in the organic phase. For the SUVs and the LUVs it has been shown that a surface gel film obtained by the evaporation of such an inverted phase can play the same role as the precursor films described above (9–12).

In this work we show that a precursor film prepared from an inverted phase can also be used for the electroformation of GUVs. We illustrate the method by incorporating chitosan, a natural polysaccharide, in the GUVs membranes. Chitosan, a polymer derived from chitin (13–15), has been recently investigated in small liposomes (10–12) and it represents a possible biocompatible and biodegradable additive for improving liposome performance in pharmaceutical or cosmetic applications (12,16,17). In particular, chitosan-containing liposomes have been shown to exhibit advantageous mucoadhesive properties (18) and to have a positive impact in liposomal formulations for burns and wounds healing (19), as well as for the gastrointestinal tract (20,21). We demonstrate here, by quantitative optical analysis, that the electroformation method applied to inverse phase precursor films containing chitosan leads to the formation of GUVs with membranes decorated with the polysaccharide. We believe that our method paves the road for further evaluation of the effect of polysaccharides on phospholipid membranes by means of well-established GUVs characterization techniques: optical techniques (1,22), elasticity by micropipette and other methods (8,23), or adhesion control by interferometry (24–26).

MATERIALS AND METHODS

Materials

Phospholipids used in this work are 1,2-dioleoyl-*sn*-glycero-3-phosphocholine (DOPC, 99%, Sigma-Aldrich, St. Louis, MO), and fluorescent 1-oleoyl-2-[12-[(nitro-2-1,3-benzoxadiazol-4-yl)amino]dodecanoyl]-*sn*-glycero-3-phosphocholine (NBDPC, 99%, Avanti Polar Lipids, Alabaster, AL), without further purification. Chitosan is low molecular mass (= 1.49 × 10^5 g/mol) as determined by light scattering (10), with a degree of deacetylation of 85% (99%, Sigma-Aldrich) and polydispersity M_w/M_n = 1.4. Fluorescein isothiocianate isomer I (90%, Fluka BioChemika, Buchs, Switzerland), chloroform (Sigma-Aldrich), fluorescein sodium salt (Sigma-Aldrich), methanol (Normapur; VWR International-Belgium,

Submitted April 13, 2008, and accepted for publication December 18, 2008.

*Correspondence: omar@iq.ufrgs.br

Editor: Peter Hinterdorfer.

0006-3495/09/04/2719/8 $2.00

doi: 10.1016/j.bpj.2008.12.3928

Leuven, Belgium), sucrose (99%, Sigma-Aldrich), glucose (99%, Sigma-Aldrich), and all other reagents, are of analytical grade.

Methods

Fluorescently labeled chitosan

Fluorescently labeled chitosan was obtained following Qaqish and Amiji (27). Chitosan was reacted with fluorescein to provide a 1:100 ratio of labeled/nonlabeled monomer assuming the average molecular mass of 1.49×10^5 g/mol. After reaction, the product was kept under stirring in methanol for 15 min, followed by an exchange of the liquid phase. This procedure was repeated several times until the methanol appeared colorless, to prevent the presence of free fluorescein. Fluorescent chitosan was then dried in a desiccator and kept in the dark.

GUVs with composite bilayers containing chitosan

We prepared giant phospholipid vesicles by a modification of the reverse phase evaporation method used, for instance, in Mertins et al. (10) for obtaining small liposomes having chitosan outside the membrane, as well as in the inner membrane surface. The method is based on the formation of an inverse phase emulsion from a mixture of a small quantity of water having chitosan and an organic solution of phospholipids. Drying the emulsion under vacuum so that a reverse micelle (gel) phase remains on the substrate, and finally rehydrating the gel layer with an aqueous solution, leads to the spontaneous formation of several bilayer structures in the solution, with a predominant fraction of LUVs. We have adapted and used this methodology to the formation of GUVs with composite bilayers containing water-soluble chitosan.

Precursor solution

Filtered solutions (0.22 μm, from Millipore, Billerica, MA) of 2.5 mg/ml (5c*) of chitosan and fluorescently labeled chitosan (see above) were prepared in 0.02 M acetate buffer/0.1 M NaCl (pH = 4.5) (28). The loss of polymer due to filtration was estimated at two-thirds using fluorimetry calibration with the fluorescent polymer. Mixtures were formed by adding 5–20 μL of the latter chitosan buffer solution to 400 μL of a chloroform solution with 1 mg/mL DOPC. The mixture was sonicated (model No. 1200 Sonicator; Branson Ultrasonics, Danbury, CT) at room temperature until it became homogeneously opalescent, typically with a sonication time of 2 min. The sonicated solutions were determined to be water-in-oil emulsions using dynamic light scattering (10). The reverse emulsion was then used as the precursor solution for the standard GUVs electroformation procedure (6–8) described below.

Electroformation

A small 10 μL drop of the emulsion was first spread on an indium tin oxyde-covered glass slide, and dried under vacuum during 30 min. Then a second identical glass plate was used to cover an incubation chamber delimited by a ring of Sigillum wax (Vitrex, Copenhagen, Denmark) and filled with a 0.095 M sucrose solution (Osmomat 030 osmometer; Gonotec, Berlin, Germany). An AC voltage of 1.5 V and 10 Hz was applied across the 1 mm chamber gap for 3 h at 22 $\pm$ 1°C. The giant vesicles were then transferred to an Eppendorf vial, and kept at rest at 4°C before use. A typical observation experiment, using an inverted optical microscope (see below), was made in an observation chamber with 20 μL of the GUVs solution dispersed in 100 μL of a 0.099 M glucose solution. The slight densities difference between the inner and outer solutions drive the vesicles to the bottom slide where they can easily be observed. The concentration of glucose is slightly larger than that of sucrose. This leads to a better-relaxed state of the vesicles in the solution. Electroformed giant vesicles of pure DOPC, prepared both from a simple DOPC/chloroform solution and from an inverse emulsion, have also been used as a reference.

Observation under an optical microscope

We used an inverted microscope model No. TE 200, with a 40× objective, and a 40× phase objective (Nikon, Tokyo, Japan). A mercury lamp provided the illumination for fluorescence experiments. A fluorescent block with filters EX 450-490 nm/BA 520 nm and a 505-nm dichroic mirror was used. Pictures were recorded via a digital camera (NDIAG 1800; Diagnostic Instruments, Sterling Heights, MI) onto the hard disk of a personal computer, with a pixel depth of eight bits. To prevent quenching of the fluorescent probe, the vesicles were first localized and observed in bright-field conditions, under low illumination. An initial series of experiments on GUVs containing fluorescent chitosan enabled us to determine the optimal experimental conditions for quantitative fluorescence measurements. We have determined the sets of values of 1), the diaphragm aperture; 2), the neutral gray filter value; and 3), the camera gain and exposure time, so as to minimize photobleaching of the fluorescent chitosan, and to maximize the signal/noise ratio of the recorded images of fluorescent vesicles. The determined set of experimental parameters was then used with all of our samples. When the fluorescence intensity appeared to be too high, as for instance for the highest levels of chitosan content, the exposure time of the camera was adjusted in the range 200–1000 ms for avoiding signal saturation. This was the only acquisition parameter modified throughout the experiments. A precision of 1 ms on the latter parameter enabled us thus to normalize, with $<1\%$ error, all our quantitative fluorescence measurements.

Quantitative fluorescence analysis of the giant vesicles

The analysis is based upon the measurement of gray level profiles of the images after subtracting the background. In practice, the average intensity I_0 per pixel of the background was first computed from the vesicle surroundings. Then, we computed the total intensity F emitted by the vesicle, $F = \sum (I_i - I_0)$, where I_i is the gray level of pixel i. We recall here also how a particular fluorescence distribution in the vesicle translates into the observed gray level image. Let $O(x, y, z)$ be the three-dimensional function describing the fluorescence distribution of the object. For instance, for a total intensity F distributed over a spherical shell, one would have

$$O(r,\theta,\phi) = F \times \left(4\pi R^2\right)^{-1}\delta(r-R),$$

with R the radius of the shell, while the same intensity F distributed inside a sphere would read

$$O(r,\theta,\phi) = F \times 3/\left(4\pi R^3\right) \text{ for } r < R.$$

The observed image $I(x, y, 0)$ in the focal plane is the convolution product (29) of the object image $O(x, y, z)$ and the point spread function of the microscope (PSF),

$$I(x,y,0) = \int dx'\,dy'\,dz'\,PSF\left(x-x', y-y', 0-z'\right)O\left(x', y', z'\right).$$

The PSF can be operationally determined for given observation conditions by scanning the function $I(x, y, z)$ for a dotlike fluorescent object, typically a fluorescent bead of suboptical size:

$$PSF(x,y,z) = \int dx'\,dy'\,dz'\,PSF\left(x-x', y-y', z-z'\right)\delta(x', y', z').$$

For our conditions, we determined experimentally that the PSF can be well approximated by the normalized cylindrically symmetric function

$$PSF(\rho,z) = \left(2\pi(0.05 + 0.17|z|)^2\right)^{-1}\exp\left\{-\rho^2/\left(2(0.05 + 0.17|z|)^2\right)\right\},$$

with $\rho = x^2 + y^2$ and all distances are measured in micrometers. Note that at each out-of-focus level the total integrated intensity is constant,

$\int 2\pi\rho d\rho PSF(\rho, z) = 1$, and that the PSF width varies linearly with the distance from the focal plane.

Calibration of polymer content on the composite giant vesicles

We determined the weight fraction of polymer on the giant vesicle bilayer by a fluorimetry calibration method based on the comparison of the fluorescence from: 1), model nanometric liposomes (11) (ranging 81–265 nm) with known amounts of the fluorophore NBDPC; 2), labeled chitosan polymer solutions with known amounts of fluorescein groups; and 3), giant vesicles containing a mixture of both species. A known amount of liposomes containing 0.1% of NBDPC fluorescently labeled phospholipids were prepared by the conventional reverse phase evaporation method (10) and then diluted to several concentrations (range of 6×10^{-5}–6×10^{-4} mg/mL of NBDPC) in MilliQ water (Millipore). The fluorescence intensities of the liposomes were recorded in a fluorescence spectrophotometer (model No. F-4010; Hitachi, Tokyo, Japan) as a function of the concentration, at wavelengths $\lambda_1 = 515$ nm and $\lambda_2 = 533$ nm, that correspond to the maximum of the emission wavelength spectra of NBDPC and of the fluorescently labeled chitosan, respectively. The same calibration was performed for solutions with known concentrations of the fluorescently labeled polymer. The variations of the peak intensities at the two wavelengths as a function of concentration could be well fitted by straight lines both for the nanometric liposomes and for the polymer. The fluorescence intensity of giant composite vesicles, prepared with the same fluorescently labeled polymer and 1% of NBDPC, was also measured by the same procedure. The phospholipids and chitosan concentrations in the giant vesicles were then extracted from the calibration curves by assuming additivity of the two different fluorescence contributions.

RESULTS AND DISCUSSION

Observation of the growth chamber under the microscope revealed a similar growth behavior for vesicles electroformed from four different types of surface precursor films 1), the usual DOPC film dried from a chloroform solution; 2), a DOPC film obtained by drying an inverse emulsion phase made from DOPC, chloroform, and buffer solution at pH 4.5; 3), a DOPC and chitosan film obtained by drying an inverse emulsion phase of DOPC, chloroform, and a chitosan in buffer solution at pH 4.5; and 4), a DOPC and fluorescent chitosan film obtained by drying an inverse emulsion phase of DOPC, chloroform, and a buffer solution of fluorescently labeled chitosan at pH 4.5. Precursor films containing the polysaccharide were prepared with different polymer contents corresponding to 0.94, 1.88, and 3.75 weight percent of chitosan in DOPC. All the precursor films gave comparable vesicle sizes and vesicle yield as evaluated by the typical sizes and abundance of vesicles in the observation chamber. In all cases the giant vesicles obtained could be easily transferred into observation chambers containing osmotically matched glucose solutions. This implies that the electroformation method successfully produces giant vesicles from precursor films made from an inverse emulsion phase. We stress that the precursor film contains here, before drying, not only the phospholipid and the organic volatile solvent chloroform as in the usual electroformation protocol, but also an aqueous phase. Our success in growing giant vesicles suggests that the presence of such a phase does not prevent, during the drying stage of the preparation, prealignment of the phospholipids by the combined action of the surface and solvent extraction.

To further investigate the localization and distribution of the added water-soluble polymer with respect to the membrane, we observed giant vesicles with added fluorescent chitosan. Fig. 1, *a* and *b*, displays the images of one vesicle observed by fluorescence microscopy and by transmission in the phase contrast mode, respectively. Fig. 1, *a* and *b*,

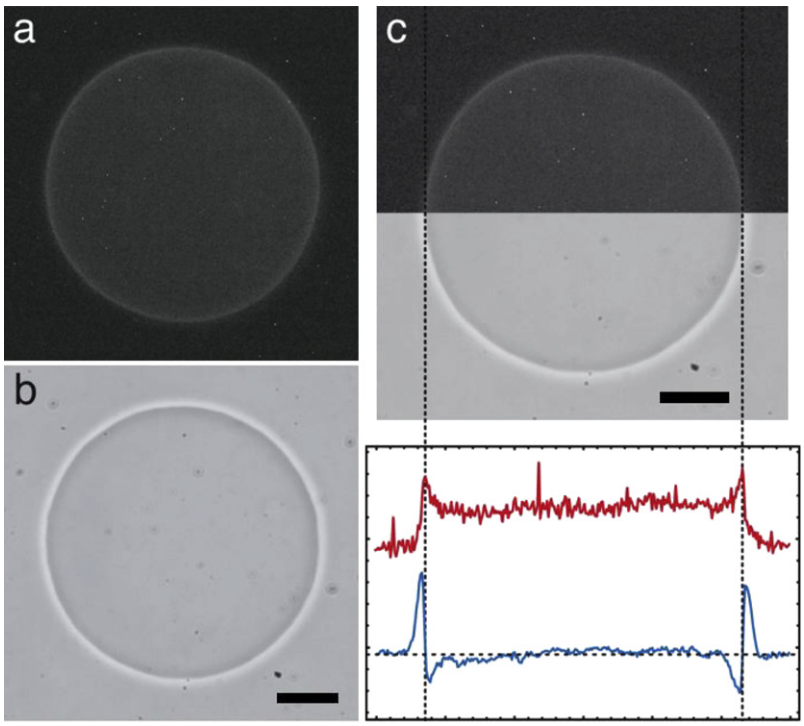

FIGURE 1 (*a*) Fluorescence microscopy image of a giant vesicle without fluorescently labeled phospholipid but with attached fluorescent chitosan. (*b*) Microscopy image of the same vesicle in the phase contrast mode and (*c*) a comparison of both images showing colocalization of the phospholipid membrane and fluorescently labeled chitosan by means of the direct comparison of the intensity profiles across the equator. In this graph, the *y* axis measures gray levels and the *x* axis corresponds to the pixels in the above images; the upper curve measures fluorescence gray levels and the lower curve phase measures the contrasting gray levels. Scale bars span 10 μm.

also shows that, with optical accuracy, the vesicle presents no pores or invaginations, and that the fluorescent polymer is evenly distributed, without any signs of phase separation. All the observed vesicles displayed similar profiles. The images show thus that this modified electroformation method leads to composite vesicles containing the polymer that had been dissolved in the aqueous solution of the inverse emulsion. Furthermore, half-sector matches and gray-level profiles for both pictures, displayed in Fig. 1 *c*, show a colocalization of both images, within optical accuracy. Such colocalization points to the presence of the polymer on the vesicle as a decoration of the phospholipid membrane, rather than encapsulated in the vesicles interior. To further investigate the polymer localization, a quantitative analysis of the polymer content of the vesicles was performed by a detailed study of the images obtained from fluorescence microscopy. We first show in the following paragraphs that the chitosan is attached to the membrane of the giant vesicles and then determine the quantity of polymer adsorbed per unit surface of the membrane.

Fig. 1 *c* shows the fluorescent gray level profile of the vesicles measured along its equator. It appears very similar to that of vesicles with a fluorescent bilayer, shown in Fig. 2, *a* and *b*. The profile is symmetric with respect to the vesicle center, with a fluorescence increase from the background value when starting away from the vesicle, leading to a maximum value at the vesicle surface and followed by a decrease toward the central region to some local minimum that is higher than the background. This profile appears qualitatively very different than the one obtained with giant vesicles encapsulating a soluble fluorophore, as shown in Fig. 2, *c* and *d*; for instance, the two intensity peaks at the membrane location seen in Fig. 2 *d* are not present in Fig. 2 *b*. A more quantitative analysis of the diametric profiles can be done if one takes into account the point spread function of the microscope. As explained in Materials and Methods, we measured the PSF of our microscope and calculated the intensity profiles expected for a vesicle with a fluorescent membrane,

$$I(x,r_0) = F\int_0^1 \frac{dt}{2\pi(0.05+0.17r_0t)^2} \times \exp\left\{-\frac{x^2+r_0^2(1-t^2)}{2(0.05+0.17r_0t)^2}\right\} \times \mathrm{BesselI}\left\{0,\frac{xr_0\sqrt{(1-t^2)}}{(0.05+0.17r_0t)^2}\right\}, \quad (1)$$

and a vesicle encapsulating a hydrophilic fluorescent species

$$I(x,r_0) = F\int_0^1 dt\int_0^{r_0} dr \times \frac{3r^2}{2\pi(0.05+0.17r_0rt)^2} \times \exp\left\{-\frac{x^2+r_0^2r^2(1-t^2)}{2(0.05+0.17r_0rt)^2}\right\} \times \mathrm{BesselI}\left\{0,\frac{xr_0r\sqrt{(1-t^2)}}{(0.05+0.17r_0rt)^2}\right\}, \quad (2)$$

where r_0 is the vesicle diameter, $x > 0$ is the distance measured on the image from the center of the profile, and t is the variable of integration. These profiles fit well our data in Fig. 2, *b* and *d*. If one assumes that the fluorescence profile in Fig. 1 *c* originates from both the surface and bulk contributions, simulations of the final profile show that contributions to the total profile from fluorophores inside the vesicle do not change the shape of the profiles significantly until the total number of bulk fluorophores reaches a few tens of percent of the number of fluorophores in the membrane. The analysis of the following paragraphs further

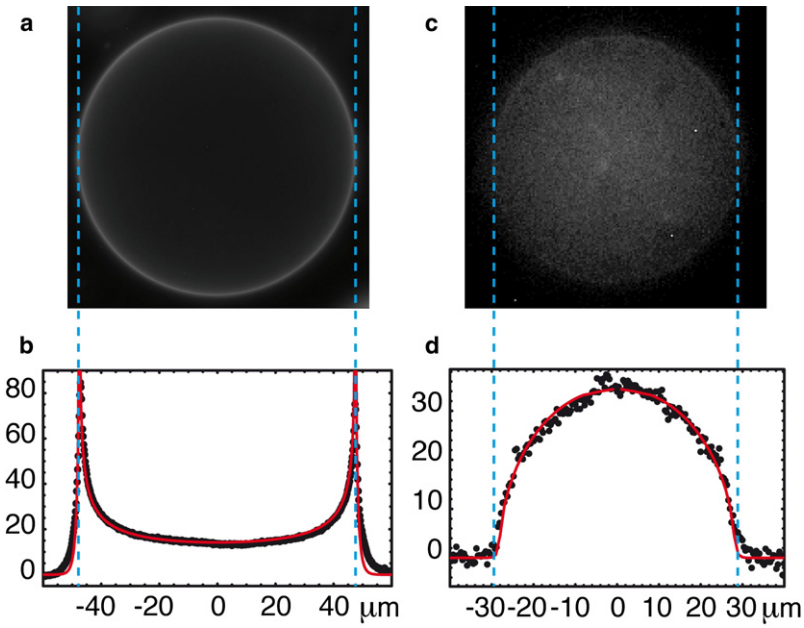

FIGURE 2 (*a*) Fluorescence microscopy image of a giant vesicle made from DOPC- and NBD-labeled phospholipids. In this case, the fluorescence is emitted by the vesicle membrane only. (*b*) The fluorescence intensity profile (*dots*) measured along the equator of image *a* and (*line*) the intensity computed from the convolution of the instrument PSF and a fluorescence distributed on the surface of a sphere. (*c*) Fluorescence microscopy image of a giant vesicle made from DOPC, with the hydrophilic fluorophore fluorescein that is homogeneously distributed inside the vesicle. (*d*) The fluorescence intensity profile (*dots*) measured along the equator of image *c* and the intensity (*line*) computed from the convolution of the instrument PSF and a fluorescence homogeneously distributed over the interior of a sphere.

confirm that the fluorescence in our composite vesicles originates from the membrane only.

In Fig. 3 *a*, we plot the value of F as a function of the vesicles area S, for several samples with different chitosan content. Error bars account for the different error sources due to background determination and accuracy of the intensity integration. The linear relation between the intensity F and the area S further confirms that the polymer is at the membrane surface. The amount of polymer-per-unit bilayer surface is therefore proportional to the intensity F. Fig. 3 *b* shows the slope $\beta = F/S$ of the different plots in Fig. 3 *a* as a function of the polymer fraction f in the precursor film. The parameter β is proportional to f, showing that the amount of the polymer on the vesicle bilayer can be tuned by the polymer content in the inverse emulsion.

The polymer attachment to the membrane can also be confirmed by the study of the stability of the composite chitosan-containing vesicles. The experimental data show that the polymer is attached to the vesicles bilayers when the original polymer solution contains well-solubilized polymer. The attraction between the polymers and the bilayers is likely to be induced by electrostatic interactions between the positive charges of the amino groups of chitosan that are obtained in the dissolution process in the low pH buffer solution, and the polar heads of DOPC, but the hydrophobic skeleton of the polymer might also interact with the hydrophobic core of the membrane (30,31). While our preparation method forces an intimate contact between the polymer and the phospholipids during the drying stage, exposure of the polymer to a free aqueous solution presents the risk of detachment of the polymer from the membrane. We have checked the stability of the polymer attachment to our composite vesicles over a period of 10 days, by monitoring the fluorescence intensity per unit surface β, measured for vesicles of different sizes by the method described above. Fig. 4 shows that within experimental uncertainties the polymer remains attached to the membranes over that period.

In the absence of more detailed information, a reasonable estimation of the amount of polymer-per-unit surface of the membrane may be provided by the simple mass fraction of polymer introduced in the precursor film. However, during the electroformation of giant vesicles, a loss or enrichment of material may occur depending on the conditions of the preparation. For instance, phospholipids and polymers may exhibit distinct transfer rates from the dried emulsion spread on the indium tin oxyde-covered glass to the GUVs. We evaluated quantitatively the amount of polymer per unit surface of the vesicles membrane by the fluorimetry calibration method described above. Recall that our method relies on the bulk measurement of the fluorescence intensity at the two wavelengths $\lambda_1 = 515$ nm and $\lambda_2 = 533$ nm that correspond to emission peaks of NBDPC and fluorescently

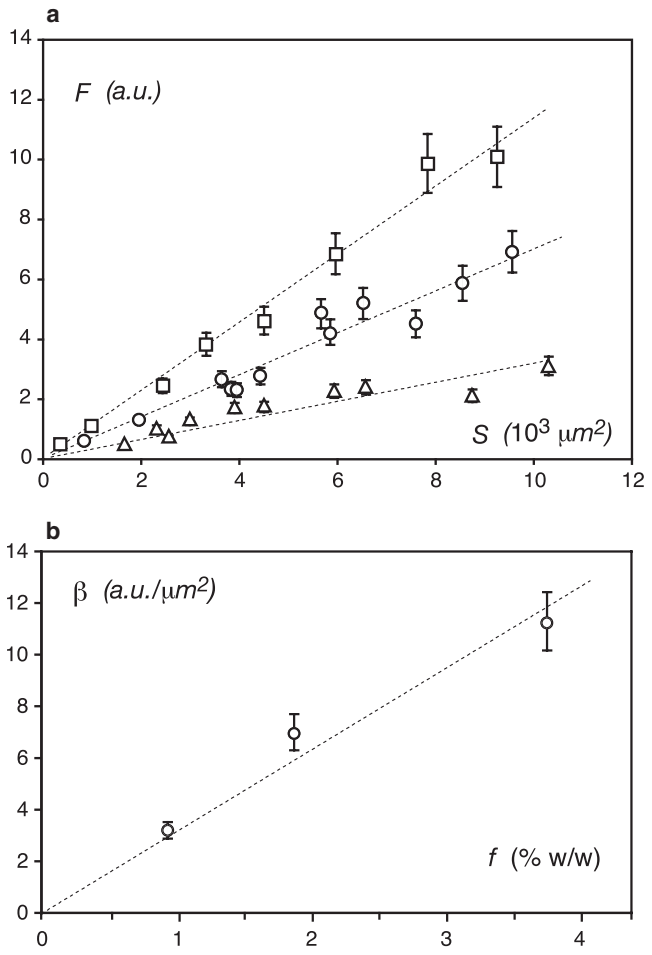

FIGURE 3 (*a*) Fluorescence intensity (F in arbitrary units) as a function of the vesicles area (S in μm^2) for three different values of the polymer weight fraction f: 0.94 (△), 1.88 (○), and 3.75 (□)% w/w chitosan. (*b*) Fluorescence intensity-per-unit surface $\beta = F/S$ as a function of the polymer fraction f.

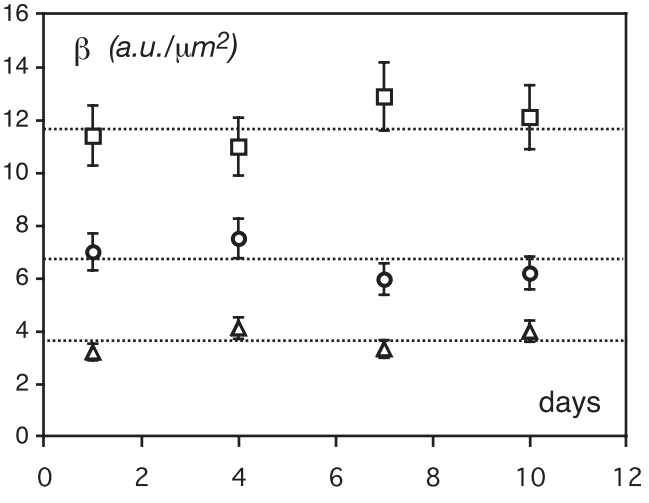

FIGURE 4 Time variation of fluorescence intensity-per-unit surface β for giant vesicles containing the three different values of the polymer weight fraction f: 0.94 (△), 1.88 (○), and 3.75 (□) % w/w chitosan. Average values of β are also indicated by a dashed line. The figure shows that the composite vesicles keep their polymer content over a period of 10 days.

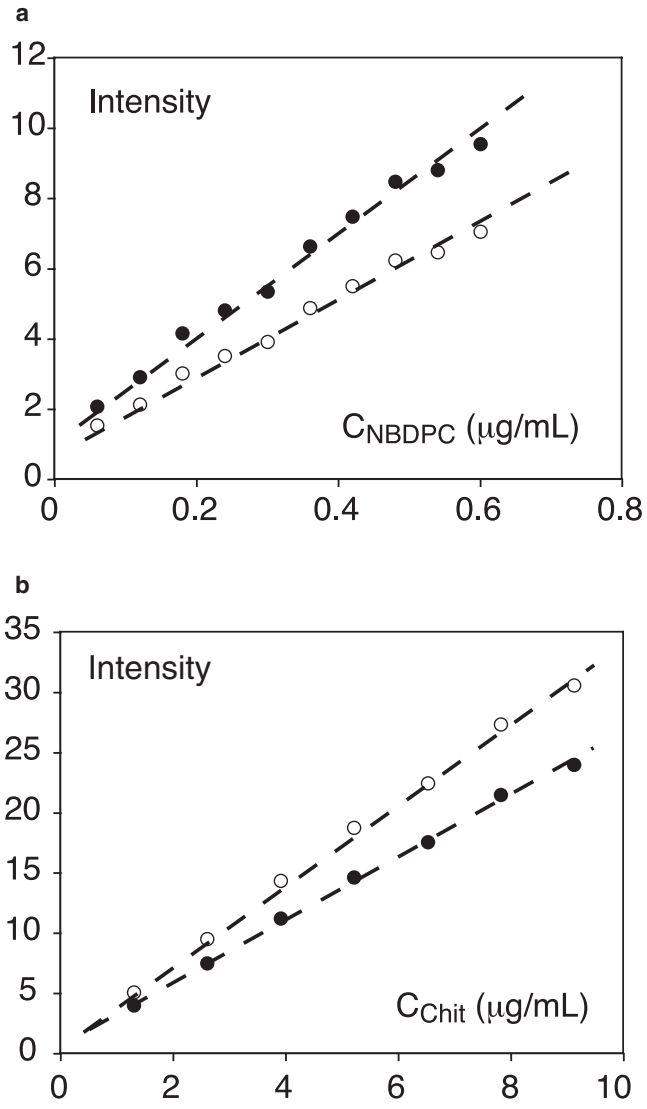

FIGURE 5 Calibration curves for determining the amount of chitosan-per-unit surface on the vesicles. The curves display emission intensities at the two wavelengths $\lambda_1 = 515$ nm (○) and $\lambda_2 = 533$ nm (•) that correspond to emission peaks of NBDPC and of fluorescently labeled chitosan.

labeled chitosan. Because those intensities vary linearly with the concentration of the two fluorescent species, as shown in Fig. 5, one simply needs to read from the calibration curves the relative values of polymer and phospholipid content in the different giant vesicles. The results revealed that giant vesicles prepared from a mixture of phospholipids and 3.75% w/w polymer exhibit a measured polymer content after electroformation of 5.7% w/w, showing that the formation method significantly enriches the polymer content of the giant vesicles. This implies that the phospholipid remaining on the surface has been depleted from its original polymer content. The measured polymer content can be translated into the conventional polymer surface excess Γ by taking an area-per-DOPC molecule of 0.725 nm^2 (32). We obtain $\Gamma = 0.1$ $mg.m^{-2}$, a typical value for polymers adsorbed on moderately attractive surfaces (33). Note that the amount of polymer-per-unit surface of the bilayer is 2 Γ. Combining results from the fluorimetry calibration and the quantitative fluorescence microscopy, one can thus assert that giant vesicles prepared from 0.94, 1.88, and 3.75% w/w polymer lead to giant vesicle membranes carrying, respectively, 0.03, 0.05, and 0.10 mg of polymer per square meter of phospholipids.

As a summary, the analysis of the fluorescence profile and of the total fluorescence combines with the stability study to confirm that chitosan is attached to the membrane of giant vesicles electroformed from a precursor film prepared from a polymer containing an inverted phase. In particular, the stability experiments clearly show that no desorption of the polymer occurs in these systems. Moreover, a quantitative calibration method provides the surface coverage values for chitosan on the DOPC membrane. Recently, the attractive interaction of chitosan and giant unilamellar vesicles has been also investigated (34) by an alternative method. The authors add a chitosan solution to a suspension of DOPC giant unilamellar vesicles and show that the polymer spontaneously adsorbs on the membrane, presumably to its external leaflet, with the adsorbed amount depending on the pH value of the solution. The electroformation method developed here does not rely on the bulk adsorption conditions for the polymer. By bringing the polymer and the membrane into intimate contact during the drying process of the precursor film, the method insures that the polymer is irreversibly attached to both leaflets of the bilayer and stays as such for at least 10 days. In future work, we plan to quantitatively compare the polymer adsorbed amounts and the stability of the polymer layers obtained by both methods. Note also that our method circumvents the typical difficulties raised by the electroformation growth of giant vesicles in a polyelectrolyte solution, where strong currents usually damage the sample and prevent vesicle growth.

Finally, in Fig. 6 we provide a synoptic table of the pathways of membrane formation mentioned in our article, comparing the classical electroformation with our modified method leading to membrane decoration both for nonspecific and specific interactions. Indeed, we would like to stress prospectively that our method is not limited to nonspecific interactions such as those acting between the amino groups of chitosan and the zwitterionic groups of the phospholipid heads, or simply between the chain backbone and the membrane water interface. Preliminary results in our group show, for instance, that the method works with specific interactions such as those promoted by the ligand-receptor couple biotin-streptavidin: repeating experiments reported in this article by simply replacing the chitosan with an equivalent concentration of fluorescent streptavidin and the phospholipids by a mixture of phospholipids and biotinylated phospholipids led to giant vesicles with fluorescent membranes, thus decorated with streptavidin, most likely on both sides of the membrane.

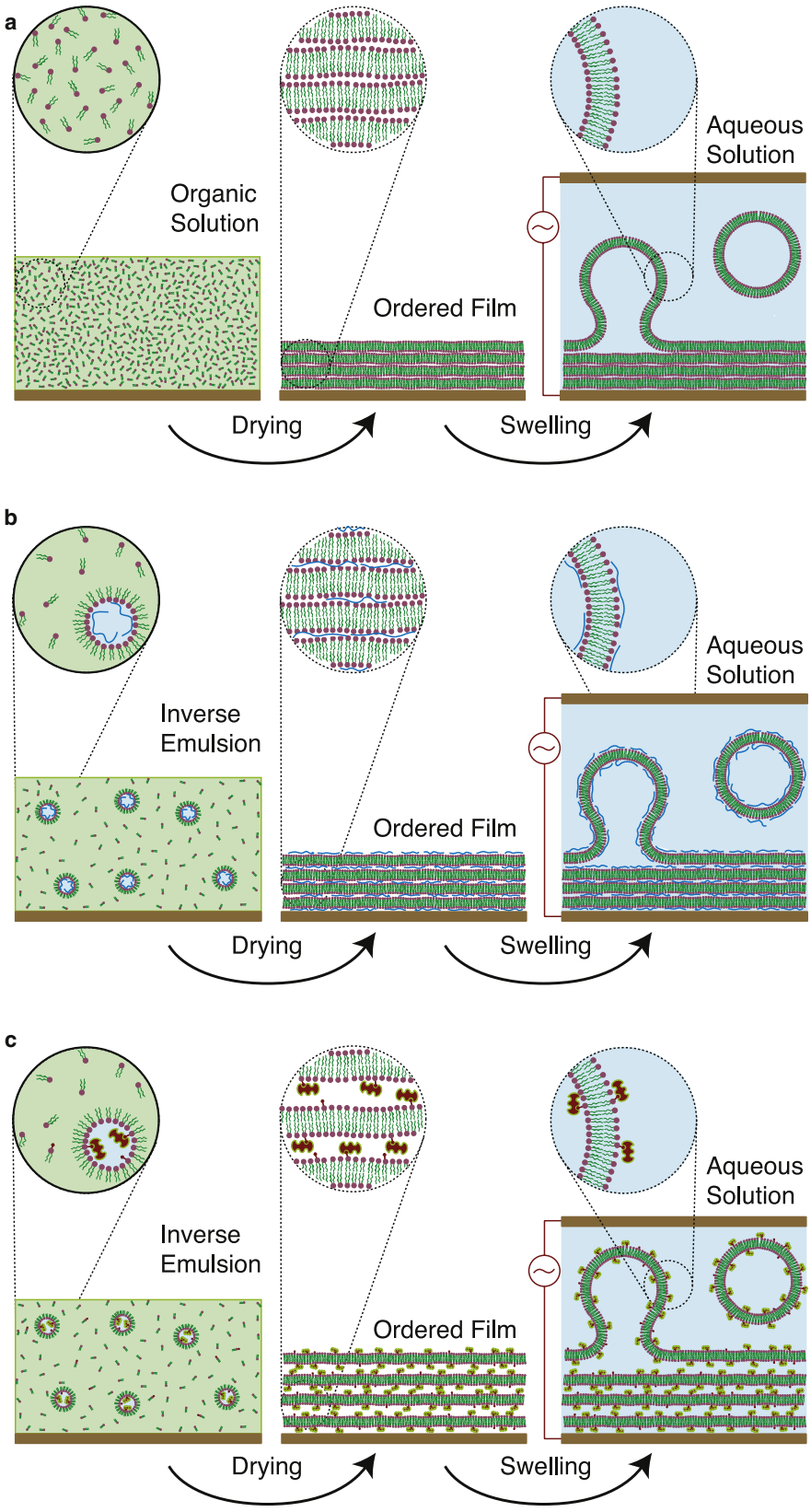

FIGURE 6 A schematic table comparing the classic electroformation method and the methods proposed in this article based on a precursor ordered film obtained from drying an inverse emulsion. (*a*) The three main steps of the classic electroformation method: 1), dissolution of the phospholipids in a volatile organic solvent, typically chloroform; 2), evaporation of the solvent and formation of an ordered film close to the surface; and 3), swelling of the film with an aqueous solution under an alternative electrical field leads to unilamellar giant vesicles. (*b*) The modified electroformation method proposed here for attaching water-soluble polymers to both sides of the giant vesicle membranes: 1), starting from an inverse phase of droplets of an aqueous polymer solution dispersed in the majority organic solvent; 2), drying the emulsion; and 3), swelling under an electric field leads to giant vesicles decorated with polymers that interact with the membrane by nonspecific interactions. (*c*) The method can also be used to decorate the membrane with water-soluble molecules that interact with the membrane by ligand receptor interactions, here schematically a fluorescent streptavidin that recognizes the biotinylated lipids of the membrane.

O.M. thanks the Coordenação de Aperfeiçoamento de Pessoal de Nível Superior/Brazil for a PhD Research Fellowship.

REFERENCES

1. Hotani, H., F. Nomura, and Y. Suzuki. 1999. Giant liposomes: from membrane dynamics to cell morphogenesis. *Curr. Opin. Colloid Interface Sci.* 4:358–368.
2. Tsumoto, K., S. M. Nomura, Y. Nakatani, and K. Yoshikawa. 2001. Giant liposome as a biochemical reactor: transcription of DNA and transportation by laser tweezers. *Langmuir.* 17:7225–7228.
3. Nieh, M. P., T. A. Harroun, V. A. Raghunathan, C. J. Glinka, and J. Katsaras. 2003. Concentration-independent spontaneously forming biomimetic vesicles. *Phys. Rev. Lett.* 91:158105.
4. Lesieur, P., M. A. Kiselev, L. I. Barsukov, and D. Lombardo. 2000. Temperature-induced micelle to vesicle transition: kinetic effects in the DMPC/NaC system. *J. Appl. Cryst.* 33:623–627.
5. Marchi-Artzner, V., L. Jullien, L. Belloni, D. Raison, L. Lacombe, et al. 1996. Interaction, lipid exchange, and effect of vesicle size in systems of oppositely charted vesicles. *J. Phys. Chem.* 100:13844–13856.
6. Angelova, M. I., and D. S. Dimitrov. 1986. Liposome electroformation. *Faraday Discuss. Chem. Soc.* 81:303–311, 345–349.
7. Luisi, P. L., and P. Walde. 2000. Giant Vesicles. . Perspectives in Supramolecular Chemistry, Vol. 6 Wiley, New York.
8. Fa, N., C. M. Marques, E. Mendes, and A. P. Schroder. 2004. Rheology of giant vesicles: a micropipette study. *Phys. Rev. Lett.* 92:108103.
9. Szoka, F. J., and D. Papahadjopoulos. 1978. Procedure for preparation of liposomes with large internal aqueous space and high capture by reverse-phase evaporation. *Proc. Natl. Acad. Sci. USA.* 75:4194–4198.
10. Mertins, O., M. Sebben, A. R. Pohlmann, and N. P. da Silveira. 2005. Production of soybean phosphatidylcholine-chitosan nanovesicles by reverse phase evaporation: a step by step study. *Chem. Phys. Lipids.* 138:29–37.
11. Mertins, O., M. B. Cardoso, A. R. Pohlmann, and N. P. da Silveira. 2006. Structural evaluation of phospholipidic nanovesicles containing small amounts of chitosan. *J. Nanosci. Nanotechnol.* 6:2425–2431.
12. Maron, L. B., C. P. Covas, N. P. da Silveira, A. Pohlmann, O. Mertins, et al. 2007. LUVs recovered with chitosan: a new preparation for vaccine delivery. *J. Liposome Res.* 17:155–163.
13. Domard, A., and M. Rinaudo. 1983. Preparation and characterization of fully deacetylated chitosan. *Int. J. Biol. Macromol.* 5:49–52.
14. Rinaudo, M., R. Auzely, C. Vallin, and I. Mullagaliev. 2005. Specific interactions in modified chitosan systems. *Biomacromolecules.* 6:2396–2407.
15. Rinaudo, M. 2006. Chitin and chitosan: properties and applications. *Prog. Polym. Sci.* 31:603–632.
16. Prabaharan, M., and J. F. Mano. 2005. Chitosan-based particles as controlled drug delivery systems. *Drug Deliv.* 12:41–57.
17. Thongborisute, J., H. Takeuchi, H. Yamamoto, and Y. Kawashima. 2006. Properties of liposomes coated with hydrophobically modified chitosan in oral liposomal drug delivery. *Pharmazie.* 61:106–111.
18. Kawashima, Y., H. Yamamoto, H. Takeuchi, and Y. Kuno. 2000. Mucoadhesive DL-lactide/glycolide copolymer nanospheres coated with chitosan to improve oral delivery of elcatonin. *Pharm. Dev. Technol.* 5:77–85.
19. Rengel, R. G., K. Barisic, Z. Pavelic, T. Z. Grubisic, I. Cepelak, et al. 2002. High efficiency entrapment of superoxide dismutase into mucoadhesive chitosan-coated liposomes. *Eur. J. Pharm. Sci.* 15:441–448.
20. Kim, H. J., C. M. Lee, Y. B. Lee, and K. Y. Lee. 2005. Preparation and mucoadhesive test of CSA-loaded liposomes with different characteristics for the intestinal lymphatic delivery. *Biotech. Biopr. Eng.* 10:516–521.
21. Thongborisute, J., A. Tsuruta, Y. Kawabata, and H. Takeuchi. 2006. The effect of particle structure of chitosan-coated liposomes and type of chitosan on oral delivery of calcitonin. *J. Drug Target.* 14:147–154.
22. Hristova, N. I., M. I. Angelova, and I. Tsoneva. 2002. An experimental approach for direct observation of the interaction of polyanions with sphingosine-containing giant vesicles. *Bioelectrochemistry.* 58:65–73.
23. Bruckner, E., P. Sonntag, and H. Rehage. 2000. Influence of toluene on the bending elastic properties of giant phosphatidylcholine vesicles. *J. Phys. Chem. B.* 104:2311–2319.
24. Radler, J., and E. Sackman. 1993. Imaging optical thicknesses and separation distances of phospholipid-vesicles at solid-surfaces. *J. Phys. II (Fr.).* 3:727–748.
25. Xiao, T., N. Fang, V. Chan, and K. Liao. 2004. A quantitative contour analysis of axisymmetric vesicles spontaneously adhering onto a substrate. *Colloids Surf. B Biointerfaces.* 34:25–31.
26. Hellberg, D., F. Scholz, F. Schubert, M. Lovric, D. Omanovic, et al. 2005. Kinetics of liposome adhesion on a mercury electrode. *J. Phys. Chem. B.* 109:14715–14726.
27. Qaqish, R. B., and M. M. Amiji. 1999. Synthesis of a fluorescent chitosan derivative and its application for the study of chitosan-mucin interactions. *Carbohydr. Polym.* 38:99–107.
28. Filho, S. P. C., and J. Desbrières. 2000. Chitin, chitosan and derivatives. *In* Natural Polymers and Agrofiber-Based Composites. E. Frollini, A. Leão, and L. H. C. Mattoso, editors. Suprema Grafica, São Paulo, Brazil.
29. Ploem, J. S., and H. J. Tanke. 2004. Fluorescence Microscopy. Royal Microscopy Society Microscopy Handbook.. No 10 BIOS Scientific, New York.
30. Radlinska, E. Z., T. Gulik-Krzywicki, F. Lafuma, D. Langevin, W. Urbach, et al. 1997. Modification of the lamellar phase in C12E5/water system by a random hydrophilic-hydrophobic polyelectrolyte. *J. Phys. II (Fr.).* 7:1393–1416.
31. Fang, N., V. Chan, H. Q. Mao, and K. W. Leong. 2001. Interactions of phospholipid bilayer with chitosan: effect of molecular weight and pH. *Biomacromolecules.* 2:1161–1168.
32. Petrache, H. I., S. Tristram-Nagle, K. Gawrisch, D. Harries, V. A. Parsegian, et al. 2004. Structure and fluctuations of charged phosphatidylserine bilayers in the absence of salt. *Biophys. J.* 86:1574–1586.
33. Fleer, G., M. C. Stuart, J. Scheutjens, T. Cosgrove, and B. Vincent. 1993. Polymers at Interfaces Springer, New York.
34. Quemeneur, F., A. Rammal, M. Rinaudo, and B. Pepin-Donat. 2007. Large and giant vesicles ''decorated'' with chitosan: effects of pH, salt or glucose stress, and surface adhesion. *Biomacromolecules.* 8:2512–2519.